J Appl Electrochem
DOI 10.1007/s10800-015-0878-0

RESEARCH ARTICLE

The influence of different pre-treatments of current collectors and variation of the binders on the performance of $Li_4Ti_5O_{12}$ anodes for lithium ion batteries

S. Wennig[1] · U. Langklotz[2] · G. M. Prinz[3] · A. Schmidt[1] · B. Oberschachtsiek[1] · A. Lorke[3] · A. Heinzel[1,4]

Received: 10 March 2015 / Accepted: 27 July 2015

Abstract In order to optimize the electron transfer between the $Li_4Ti_5O_{12}$-based active mass and the current collector, the surface of aluminum foil was modified either by alkaline etching or by a carbon coating. The as-modified aluminum foils were coated with an active mass of $Li_4Ti_5O_{12}$ mixed with polyvinylidene fluoride, sodium carboxymethyl cellulose, or polyacrylic acid as binders. Untreated aluminum and copper foils served as reference current collectors. The corrosion reactions of aluminum foil with the applied binder solutions were studied and the electrode structure has been analyzed, depending on the binder. Finally, the electrochemical performance of the prepared electrodes was investigated. Based on these measurements, conclusions concerning the electrical contact between the different current collectors and the active masses were drawn. The energy density of the $Li_4Ti_5O_{12}$ electrodes cast on carbon-coated aluminum foils was significantly increased, compared to the corresponding electrodes with a copper current collector.

Keywords Lithium ion battery · Lithium titanate · Carbon-coated current collectors · Polyvinylidene fluoride · Aqueous binder · Screen printing

✉ S. Wennig
s.wennig@zbt-duisburg.de

[1] The Fuel Cell Research Center, ZBT Duisburg, Carl-Benz-Str. 201, 47057 Duisburg, Germany

[2] Institute of Material Science, Dresden University of Technology, Helmholtzstr. 7, 01062 Dresden, Germany

[3] Experimental Physics and CENIDE, University of Duisburg-Essen, Lotharstr. 1, 47057 Duisburg, Germany

[4] Chair of Energy Technology and CENIDE, University of Duisburg-Essen, Lotharstr. 1, 47057 Duisburg, Germany

1 Introduction

In recent years, a lot of efforts were made to increase the energy density, the power density, and the cycle lifetime of lithium ion batteries to meet the growing demand for storage devices for mobile and stationary applications [1, 2]. In this context, the focus is mainly set to the development of electrochemically active cathode and anode materials. Among these, lithium titanate (LTO), $Li_4Ti_5O_{12}$, is a promising candidate as a safe and highly cycling-stable anode material due to its high reversibility of the intercalation reaction [3], excellent Li^+ mobility [4], marginal volume changes during intercalation and deintercalation [5], electrode potential of about 1.55 V versus Li/Li^+ [3], resulting in the almost complete absence of a solid electrolyte interface (SEI) [6, 7], and the prevention of lithium plating on the electrode surface [7, 8].

The drawback of LTO is the low electronic conductivity of the lithium poor configuration $Li_4Ti_5O_{12}$ [9, 10]. Various approaches to overcome this problem by modification of the active materials properties are attempted [11–14].

However, the influence of the binders or current collectors on the performance of LTO anodes is barely investigated. These components mainly influence the electrical contact between the active mass and the current collector as well as the interparticular contact, while the active material modifications improve only the intrinsic conductivity of LTO. By improving the electrical contact between the active coating and the current collector as well as between the particles, a superior performance of the electrode can be expected.

Currently, the electrodes in commercial lithium ion batteries are usually prepared using polyvinylidene fluoride (PVDF) binder and *N*-methyl-2-pyrrolidone (NMP) solvent [15]. Both chemicals are expensive and NMP is toxic.

Published online: 08 August 2015

Alternatively, water-soluble binder systems that are cheaper and environmentally friendly are being investigated. Promising binder candidates are sodium carboxymethyl cellulose (Na-CMC) [16–22] and poly acrylic acid (PAA) [23 26]. In general, an improved electrode performance is achieved by applying both aqueous binders compared to the corresponding electrodes with a PVDF binder. This effect is mainly explained by the more homogenous and compact electrode structure [18–23].

The development of cheap and lightweight current collectors with a good electrical contact to the active mass received yet less attention than the investigation of innovative binder systems. However, the energy density of the electrode can be significantly increased by using lightweight current collectors. Furthermore, the cost of lithium ion battery electrodes can be reduced by using a cheap current collector material [27]. Considering these facts, aluminum is the ideal current collector material for application in the potential range above 0.3 V versus Li/Li^+ [27, 28]. Notwithstanding, the electrical insulating passive film spontaneously formed on the aluminum surface increases significantly the electrical resistance to the active mass [29]. The surface pre-treatment of aluminum is a promising strategy to overcome this problem. One approach is the impregnation of the aluminum with carbon coatings, either by vapor deposition [30, 31], or by tape casting of a slurry [32]. Due to the enhanced electrical contact between the current collector and the active mass, the electrode performance is improved. However, the described methods are either expensive [30, 31] or environmentally unfriendly chemicals [32] are used for the surface treatment. In addition, the origin of the improved contact resistance is still not clarified. Moreover, the influence of the applied binder on this electrical contact has not been investigated so far.

Therefore, the present work intends to elucidate the interactions between differently pre-treated aluminum current collectors and binder systems. The effect of the binder and the applied pre-treatment of the current collectors on the structure-property relationship of LTO electrodes was investigated. For this purpose, five different current collectors were adopted, including untreated aluminum foil (Al), etched aluminum foil (Al etched), carbon black-coated aluminum foil (Al CB), graphene nanoplatelets-coated aluminum foil (Al GnP), and copper foil (Cu). Therein, the untreated copper, which is a common current collector for LTO anodes [11–13, 33], and the untreated aluminum served as reference. The coatings consisted of the environmentally friendly Na-CMC as a binder and carbon black (CB) as well as graphene nanoplatelets (GnP) as conductive additives. They were applied by a cheap and efficient screen printing process. Subsequently, the corrosion reactions of aluminum with the different binder solutions were investigated by inductively coupled plasma optical emission spectroscopy (ICP-OES) and infrared (IR) spectroscopy. Finally, anodes were produced using different current collectors and active coatings containing LTO and PVDF, Na-CMC or PAA as a binder. Their electrochemical performance was investigated and complemented by physical analysis. Based on these measurements, conclusions concerning the electrical contact between the active mass and the current collector were drawn.

2 Experimental

2.1 Pre-treatment of current collectors

The aluminum foil was firstly treated by etching in a 2 M KOH solution for 5 min at room temperature. Alternatively, untreated aluminum was coated with carbon-based slurries. The slurries contained carbon black (Super-P Li^{TM}, Timcal) and graphene nanoplatelets (xGnP® M-25, XG Sciences), respectively, as conductive additives. Na-CMC (Walocel CRT 2000 PA, Dow Chemicals) served as a binder, while deionized water, 2-propanol (VWR BDH Prolabo®, AnalaR Normapur, absolute), and ethane-1,2-diol (Mallinckrodt Baker, analyzed reagent) were used as solvents. CB was used as-delivered, whereas the GnPs were dried under vacuum before using. To prepare the CB slurry, firstly Na-CMC (2.5 wt%) was dissolved in deionized water (97.5 wt%). Subsequently, CB was added and the resulting suspension was homogenized by means of sonication. To realize homogenous GnP slurries, a mixture of deionized water (53 wt%), 2-propanol (42 wt%), and ethane-1,2-diol (5 wt%) was adopted as solvent. Na-CMC (1.7 wt%) was dissolved in this solvent mixture (98.3 wt%). Afterwards the GnPs were added and the dispersion was sonicated. Both slurries were screen printed onto aluminum with an EKRA E1-II (Asys Group) screen printing machine. Finally, the samples were dried under vacuum for 12 h at 170 °C. The obtained adhesion layers were composed typically of conductive additive (83 wt%) and Na-CMC (17 wt%), corresponding to average mass loadings of 0.2 mg cm^{-2} CB and 0.3 mg cm^{-2} GnP, respectively.

2.2 Electrode preparation

Commercial LTO powder (T2, Clariant) was used as an electrochemically active material. Carbon black (Super-P Li^{TM}, Timcal) served as a conductive additive. Three different polymer binders were used for the electrode fabrication: (i) PVDF (Solef® 1013, Solvay Solexis), (ii) Na-CMC (Walocel CRT 2000 PA, Dow Chemicals), and (iii) PAA (25 wt% dissolved in water, average M_w 240,000 g mol^{-1}, Alfa Aesar®).

PVDF was dissolved in NMP (Acros Organics, AcroSeal® extra dry, water <50 ppm) by continuous magnetic stirring for 2 h at room temperature. Na-CMC was dissolved in a mixture of deionized water (80 wt%) and ethanol (20 wt%, VWR BDH Prolabo®, AnalaR Normapur, absolute) by magnetic stirring overnight at room temperature. The PAA solution was obtained as the polymer was dissolved in a mixture of deionized water (80 wt%) and ethanol (20 wt%) for 10 min at room temperature. Afterwards, carbon black was added to each of the binder solutions and the resulting dispersions were homogenized by ultra-sonication. After addition of LTO, each of the suspensions was dispersed with a turbo mixer for 1 h. The resulting slurries were cast on the different current collectors by using an adjustable doctor blade (film width: 50 mm). Subsequently, the electrodes were pre-dried for 8 h at a temperature of 90 °C under vacuum. Finally, circular electrodes with a diameter of 12 mm were laser-cut and dried at 90 °C for 24 h under vacuum.

The final composition of the electrodes amounted to LTO (90 wt%), carbon black (5 wt%), and binder (5 wt%). The average mass loading of LTO was between 2.2 and 2.7 mg cm^{-2}.

2.3 Physical characterization

Scanning electron microscopy (SEM) images were recorded with a FEI Helios Nanolab™ 600 by applying an acceleration voltage of 5 kV. The surface roughness of the current collectors was determined with a confocal microscope (NanoFocus, µsurf custom).

2.4 Chemical analysis

Aluminum was exposed to various aqueous binder solutions and deionized water as a reference. The PAA and Na-CMC concentrations were set to 1 wt% in all binder solutions. The pH value of these binder solutions was determined by a pH test paper. A three-neck flask was filled with the described solutions and the aluminum foil was added. The suspensions were stirred and refluxed at a temperature of 90 °C for 24 h. Subsequently, they were filtrated and the aluminum amounts in the solutions were determined via ICP-OES (Thermo Elemental Intrepid HR). In addition, the leached aluminum foils were investigated via IR spectroscopy in ATR (attenuated total reflection) configuration, using a Nicolet™ is™ 10 FT-IR spectrometer.

2.5 Electrochemical tests

Electrochemical measurements were carried out using Swagelok®-type three electrode cells. Lithium foil (Chemetall, 100 µm thick) served as counter and reference electrode, and polypropylene fleeces soaked with electrolyte were used as separator. The electrolyte was a solution of 1 M $LiPF_6$ in ethylene carbonate and dimethyl carbonate (1/1, *m/m*). The test cells were assembled in an argon-filled glove box.

Galvanostatic (GC) and cyclic voltammetry (CV) measurements of the LTO anodes were performed with a Basytec CTS Lab XL battery tester. GC experiments were carried out in the range of 1.0–2.0 V versus Li/Li^+, applying various currents which correspond to C rates between 1/20 and 16. The GC measurements were carried out as a triple determination, and the average values of the capacities and energy densities are shown as representative results. The CVs were recorded between 1.0 and 2.0 V versus Li/Li^+ with a scan rate of 10 µV s^{-1}. The CVs of the current collectors were recorded with a BioLogic VMP 3 potentiostat between 1.0 and 2.0 V versus Li/Li^+ with a scan rate of 10 µV s^{-1}. All CVs were repeated at least once.

3 Results and discussion

3.1 Physical characterization of current collectors

Figure 1 shows SEM images of carbon-coated aluminum using (a) carbon black and (b) graphene nanoplatelets as conductive additive. In Fig. 1a, a homogeneous carbon black network with a thickness of ca. 3 µm is visible. The observed breaking edge between the coating and the current collector was most likely generated during the sample preparation for the SEM measurement. In the GnP coating, the graphene flakes are mostly arranged parallel to the aluminum surface, with only few protruding flakes (Fig. 1b). The thickness of the GnP layer is approximately 1 µm.

Figure 2 shows exemplary 3-D illustrations of the surface topologies of (a) untreated and (b) GnP-coated Al foil, measured by confocal microscopy. At the top of both figures, a 2-D illustration of the respective surface topology is depicted. Untreated aluminum has a smooth surface with well-ordered grooves caused during the foil production process (Fig. 2a). After coating the foil with the GnP slurry, the texture changes significantly (Fig. 2b). The dark areas (up to 2.5 µm) can be assigned to flatly ordered graphene flakes, whereas the light-colored arrays (from 2.5 till 17.5 µm) can be related to vertically arranged graphene flakes bulking out the surface. These protruding flakes form elevations of up to 20 µm which cannot be observed in the SEM images. However, the area scanned by confocal microscopy was about two orders of magnitude larger compared to those obtained from the SEM measurement. Thus, both techniques address morphological features of completely different scale.

Based on these surface topologies, the ratio between the geometric (A_{geom}) and the real surface area (A_{real}) of the

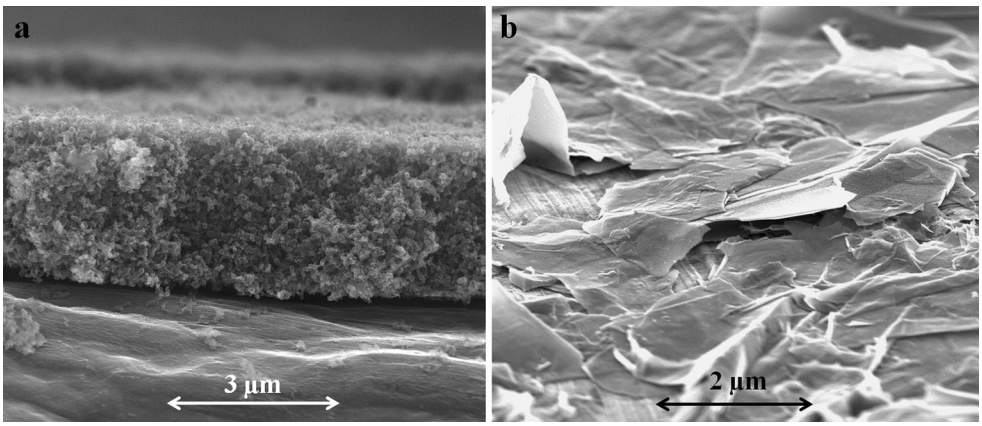

Fig. 1 SEM images of aluminum foils coated with **a** CB and **b** GnP as conductive additive

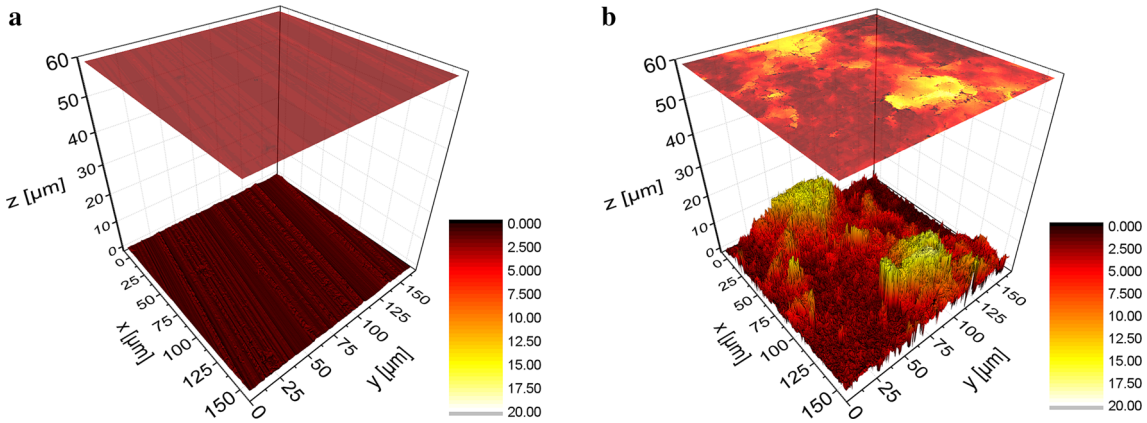

Fig. 2 3-D illustration of surface topologies of **a** untreated aluminum foil and **b** aluminum foil coated with GnP/Na-CMC. At the top of each figure a 2-D illustration of the surface topology is shown

different current collectors was calculated (Table 1). Blank metal foils have very smooth surfaces (see Fig. 2a). The surface roughness of Al is just slightly increased by the etching, but significantly modified by the screen printed coating. The application of the conductive coatings increases the surface roughness by the factor two (CB) and ten (GnP), respectively.

3.2 Electrochemical characterization of current collectors

Figure 3 shows CVs of the current collector foils, which are representative for the materials. In the case of both blank metal foils, there is one distinct reduction peak at a potential of about 1.45 V versus Li/Li$^+$ in the first cycle. It was assigned to the reduction of trace oxygen dissolved in the electrolyte [34]. There are no notable differences between untreated copper and aluminum. In contrast, the carbon-coated current collectors show cathodic currents at potentials below 1.6 V versus Li/Li$^+$. One hypothesis is that the oxygen reduction observed at pure metals was probably kinetically hindered on the carbonaceous surfaces. This resulted in a broadening of the reduction peak and a shift in cathodic direction. However, there are still distinct currents flowing in the second cycle. Thus, a decomposition of trace impurities is rather unlikely. However, in the potential range below 1.3 V versus Li/Li$^+$, an electrochemical decomposition of the electrolyte is also possible [34]. The according overpotential depends on the surface state. Consequently, the electrolyte decomposition might be enhanced at carbon surfaces as carbon offers a variety of reactive surface states that influence the reaction with the electrolyte components [35, 36]. The according

Table 1 Relation between the geometric and real area of different collectors (referred to the scale of the optical measurement)

Current collector	Al	Al etched	Al CB	Al GnP	Cu
A_{real}/A_{geom}	1.0	1.1	2.2	10.5	1.0

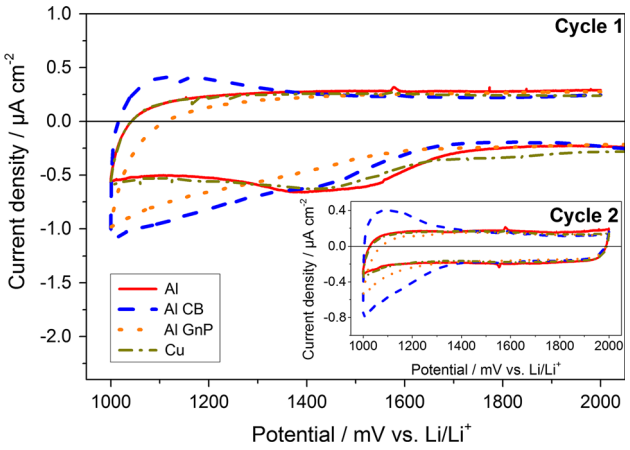

Fig. 3 CVs of various current collector foils in a potential range of 1.0–2.0 V versus Li/Li^+

reactions are at least partially reversible when using carbon black-coated current collectors, as anodic currents were measured in the back sweep. The reversible capacity contribution of the carbon black-coated aluminum foil is in the range of 5 µAh cm^{-2}. It is possible that Li^+ interacted electrochemically with CB, resulting in a slight reversible capacity contribution [37].

The electrolyte decomposition was presumably the cause of the SEI formation. The decrease of the current density in the second cycle indicated the formation of such layer. The SEI formation is generally anticipated at potentials below 1 V versus Li/Li^+ [6, 38]; however, even at potentials above 1 V versus Li/Li^+, the formation of a thin surface film has been observed [39, 40]. Such a SEI-like film might not be densely closed, which explains the residual currents detected in the CVs.

To conclude, the electrolyte is stable at the redox potential of $Li_4Ti_5O_{12}$ (1.55 V vs. Li/Li^+) [3, 6]. However, by cathodic cycling below 1.3 V, the electrolyte is decomposed on the surface of the respective current collectors and a SEI-like film is formed. Furthermore, the measured reversible capacity contribution of the carbon black-coated aluminum foil is negligible. Hence, the use of carbon-coated current collectors should not cause additional parasitic side reactions, disturbing the electrode reaction and declining the electrode's performance.

3.3 Corrosion reactions of aluminum with aqueous binder solutions

Vedder et al. report about the dissolution of the passive layer of aluminum being composed of a dense layer of amorphous Al_2O_3 in liquid water and the subsequent formation of AlOOH on the metal surface [41]. This AlOOH-layer is described as porous and amorphous. Its thickness is in the micron-range, depending on the time and the temperature.

To investigate the influence of the polymer on the chemical reaction between aluminum and water, the pH value of the binder solutions was determined and ICP-OES measurements as well as IR investigations were performed. The treatment of aluminum in pure deionized water served as a reference. In contrast to aluminum, copper is inert in water. Thus, these experiments were not conducted with Cu foil.

The pH values of the different solutions are listed in Table 2. The pH of deionized water is weakly acidic. Na-CMC reacts alkalescent in water and the PAA solution is acidic. Additionally, Table 2 shows the results of the ICP-OES analysis. Generally, aluminum is found in different liquid media indicating a chemical reaction between aluminum and the corresponding solutions. The highest amount of aluminum is observed in the deionized water, followed by the Na-CMC solution and the lowest amount is noted in the PAA solution. Thus, Na-CMC and PAA influence the aluminum–water reaction. To study the impact of the applied polymer onto the properties of the aluminum surface, IR spectra of the leached aluminum foils were recorded (Fig. 4).

The sample which was treated with pure water exhibits a number of characteristic bands for aluminum hydroxides and oxyhydroxides. The bands at wavenumbers 3546, 3455, 3418 cm^{-1}, as well as 1012 and 973 cm^{-1} were related to literature values of γ-$Al(OH)_3$ (Gibbsite) [42], while the bands at 757 and 625 cm^{-1} and the shoulder at about 550 cm^{-1} were assigned to Boehmite (γ-AlOOH) [42].

According to the results from the ICP-OES analysis and the investigations of Vedder et al. [41], the substitution of Al_2O_3 by an aluminum hydroxide/oxyhydroxide layer is observed when aluminum was exposed to liquid water.

On the contrary, the spectra of aluminum treated in both polymer solutions show additional features of the respective binder species. In case of the sample treated in the PAA solution, the absorbance of the passive layer is significantly lower compared to the other samples. This is an indication for a thinner surface film compared to the other aluminum foils, although it could not be used as a quantitative measurement of the film thickness. The modes between 1600 and 1300 cm^{-1} were assigned to carboxylic C–O–bonds. According to the absence of the C=O stretching band, this polymer was not present in its acidic form. In accordance with the literature, this effect can be explained by the linking of the polymer to the aluminum surface by the carboxyl groups [43–45]. Additionally, the bands for AlOOH or $Al(OH)_3$ are not visible in this spectrum, which can be explained by the pH value. In contrast to the formation of aluminum hydroxide/oxyhydroxide in a weakly acidic environment, at a pH of about 3, the amphoteric Al_2O_3 presumably reacts to water and Al^{3+},

Table 2 pH values of different solutions and aluminum amounts in these media determined by ICP-OES

Solution	Deionized water	Aqueous Na-CMC solution	Aqueous PAA solution
pH value	6.2	6.5	3–3.5
Al amount	3295 mg l^{-1}	1128 mg l^{-1}	384 mg l^{-1}

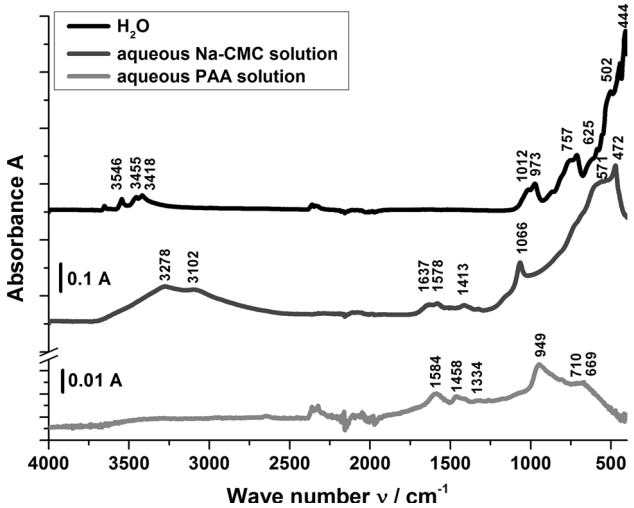

Fig. 4 FT-IR spectra of aluminum foils treated in water and aqueous binder solutions of Na-CMC and PAA

which are linked to the polymer. So the authors suggest that the aluminum(III)-polyacrylate formation was favored over the hydroxide/oxyhydroxide precipitation. This explains the decreased aluminum amount in presence of PAA in the solvent.

The spectrum of aluminum which was treated in the Na-CMC solution shows various bands dedicated to γ-AlOOH, e.g., at 3278, 3102, and 1066 cm^{-1}, but no characteristic bands of Gibbsite [42]. After the addition of the Na-CMC binder into water, the passive film on aluminum changes its composition and becomes rather an oxyhydroxide than a hydroxide layer. Additionally, similar to the PAA solution, several modes between 1700 and 1300 cm^{-1} are visible, which can be assigned to carboxylic C–O-bonds, too. Hence, Na-CMC was linked to the metal surface. The aluminum amount in the Na-CMC containing solution (see Table 2) lies between those of pure water and the PAA solution. Hence, Na-CMC prevented partially the aluminum–water reaction; e.g., the aluminum surface was blocked by Na-CMC, thus hindering the hydroxide or oxyhydroxide deposition. However, the protective effect was less distinct than with PAA, because the precipitation of aluminum hydroxide/oxyhydroxide cannot be prevented effectively at a pH of about 7.

Aqueous binder systems are obviously able to remove the initial passive layer on the aluminum foil, depending on the applied polymeric binder. Therefore, the authors assume that the electrical contact between the active mass and aluminum could be enhanced by using an aqueous binder system. Due to the chemical stability of the native passive layer toward NMP/PVDF, the worst electrical contact between aluminum and the active mass might occur with this binder. The electrochemical performance of LTO electrodes with the PVDF binder should be improved by a carbon coating of aluminum.

To conclude, electrochemical measurements of LTO electrodes composed of different binders and current collectors were performed to survey these assumptions. Based on these results, it was evaluated if copper could be really substituted by carbon-coated aluminum current collectors.

3.4 Characterization of LTO electrodes

3.4.1 Reference system (PVDF binder): comparison of untreated Cu versus Al

First of all, the performance of LTO electrodes processed as usually, using PVDF binder as well as NMP as a solvent and cast on untreated aluminum and copper, has to be understood. Figure 5a shows CVs of such electrodes. The discharge curves at three different C rates are displayed in Fig. 5b.

The observed peaks in the CVs could be assigned to the lithiation–delithiation reactions of $Li_4Ti_5O_{12}$ (Eqs. 1 and 2):

$$Li_4Ti_5O_{12} + 3Li^+ + 3e^- \overset{red}{\rightarrow} Li_7Ti_5O_{12} \quad (1)$$

$$Li_7Ti_5O_{12} \overset{ox}{\rightarrow} Li_4Ti_5O_{12} + 3Li^+ + 3e^- \quad (2)$$

These electrochemical reactions go along with a two-phase transformation among the spinel structure of $Li_4Ti_5O_{12}$ and the rock-salt structure of $Li_7Ti_5O_{12}$ [3, 10]. The electrical conductivity of $Li_4Ti_5O_{12}$ is very low (10^{-13} S cm^{-1}) [46]. In contrast, $Li_7Ti_5O_{12}$ is a good electronic conductor due to the existence of the mixed valence state of titanium [47, 48]. During lithiation, the formation of the conductive $Li_7Ti_5O_{12}$ starts at the surface of the $Li_4Ti_5O_{12}$ particles and proceeds to their core. During delithiation, in turn, electrical insulating $Li_4Ti_5O_{12}$ is formed on the particle surface. Consequently, the delithiation is kinetically hampered by the low electronic conductivity of the particle shells, causing a charge transfer limitation [49].

In case of the electrode cast on copper, the CV shows narrow reduction and oxidation peaks at 1.53 V versus

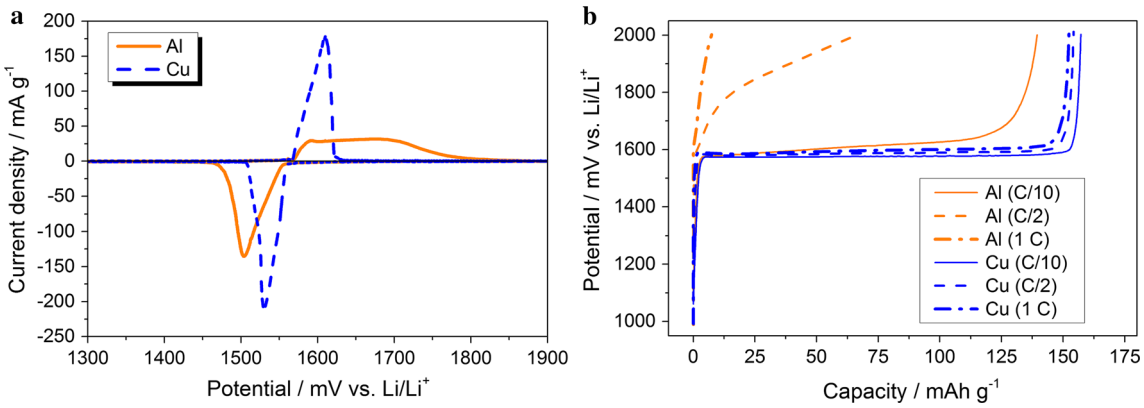

Fig. 5 Electrochemical behavior of LTO anodes with PVDF binder using untreated Al and Cu as current collector: **a** cyclic voltammograms (CV), **b** discharge curves at different C rates (the applied C rate is declared in brackets)

Li/Li^+ and 1.61 V versus Li/Li^+, respectively, indicating fast electrochemical reactions. However, the shift of the oxidation peak related to the equilibrium potential of LTO (1.55 V vs. Li/Li^+ [3]) is more distinct as the shift of the reduction peak, which can be accounted to the reaction mechanism of the active material.

Using aluminum as current collector, the redox reaction is kinetically hindered, as it is obvious from the shift of the peak potentials and especially by the extreme broadening of the oxidation peak. Hence, a significant electric resistance seems to exist in this electrode, limiting the performance compared to an anode cast on copper. As the active coating and the conditions of the measurement were identical, the difference must arise from the current collector material. Indeed, aluminum is covered by an electrically insulating passive layer [29, 41] impeding the electron flow between the active coating and the current collector. Also copper forms a thin oxide film on its surface, but in contrast to aluminum, this copper oxide film is semiconducting [29]. Thus, the authors suggest that on copper, no electrical insulating layer hampered the electron transfer between the active mass and the current collector. Hence, the electrical insulating layer of aluminum was responsible for the sluggish kinetics. Due to the reaction mechanism of LTO, the oxidation was even more affected than the reduction.

The discharge curves (see Fig. 5b) of the LTO electrodes with a PVDF binder confirm the results of the CVs. Flat voltage profiles for the anode cast on copper at C/10, C/2, and 1 C are obtained. The observed capacities are 157, 154, and 152 mAh g^{-1}, respectively. For the sample applied on untreated aluminum, a flat voltage profile is only observed at C/10, but the capacity is about 20 mAh g^{-1} lower compared to the electrode with a copper current collector. The increase of the C rate to 1/2 leads to a severe capacity decrease and the discharge potential is drastically raised indicating a large overvoltage. A further increase up to 1 C causes a dramatic capacity drop to less than 10 mAh g^{-1}.

Hence, the electrochemical performance of the anode with untreated aluminum was apparently limited by the large overvoltage. As discussed in the CVs, the major influence on the overvoltage was due to the ohmic resistance between active mass and aluminum, generated by the electrical insulating layer on the metal surface. To sum up, the authors' experiments approved that untreated aluminum is not applicable as a current collector for LTO anodes with a PVDF binder.

3.4.2 *Influence of the pre-treatment of current collectors (PVDF binder)*

In a second step, the advantageous effect of pre-treating the aluminum current collectors on the electrode performance should be validated. The capacity retention of LTO anodes, processed with PVDF in NMP and cast on differently pre-treated current collectors, at different C rates is shown in Fig. 6a. The cycling test started with a formation sequence at low C rates (1/20 up to 1/2), followed by a stability test over 75 cycles applying 1 C and a subsequent rate capability test up to 16 C.

The simplest way to pre-treat the aluminum surface is by alkaline etching. In this way, the capacity retention can already be improved compared to the anode with untreated aluminum (see Fig. 5b). At 1 C, the capacity is still 140 mAh g^{-1}. By the alkaline etching of the aluminum foil the amphoteric Al_2O_3 was removed. However, the passive film reformed after the pickling, but its thickness decreased distinctly compared to untreated aluminum due to the short delay (1–2 min) up to the beginning of the coating process. Consequently, the resistance of the oxide film was reduced, and thus, the electrical contact to the active layer was improved and the electrode performance enhanced. However, the capacity is extremely reduced at C rates $\geq$2.

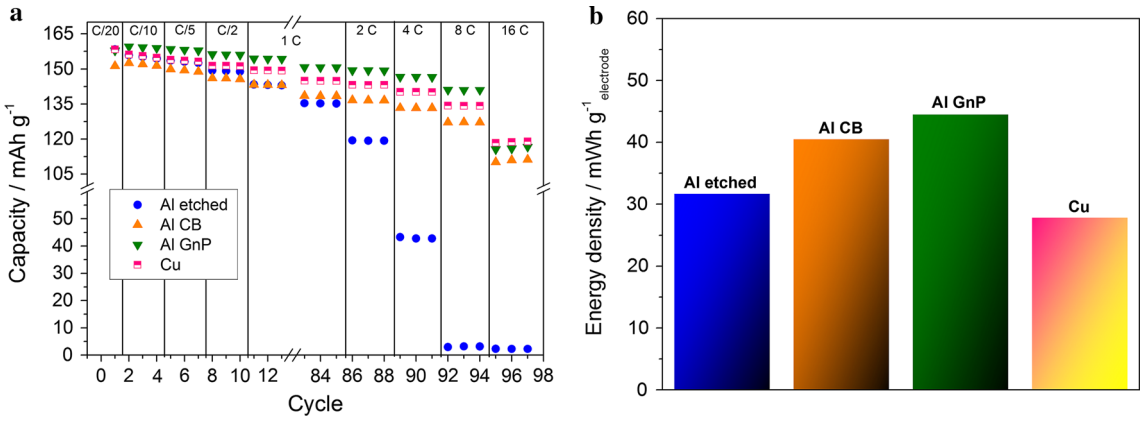

Fig. 6 Electrochemical performance of LTO electrodes with PVDF binder using different current collectors, **a** capacity retention at different C rates, **b** specific energy density at 2 C, referred to the whole mass of the electrode (including the weight of the current collector)

Hence, this method of surface modification is not suitable to obtain high-rate capable anodes.

A remarkable improvement is achieved by implementation of a carbonaceous layer between the active mass and the aluminum foil. As a result of this treatment, the rate capability of the electrodes is massively enhanced. Generally, a discharge capacity of more than 100 mAh g^{-1} even at 16 C is observed, when the aluminum was pre-coated. Thus, the capacity and the rate capability of electrodes with carbon-coated aluminum foils are comparable to electrodes cast on copper. However, by substituting the heavy copper current collector by innovative, lightweight carbon-coated aluminum foils, the energy density of LTO anodes with a PVDF binder can be enhanced by about 59 % (see Fig. 6b).

As discussed above, in the course of the carbon coating on aluminum, the initial oxide film was dissolved and so a reformation of the oxide layer was prevented. Consequently, the electrical contact between the active mass and the current collector was significantly enhanced. An improved high rate capability of LTO anodes using carbon-coated aluminum is also described by Wu et al. [30]. Notwithstanding, to the best of the authors' knowledge in our work, a cheap and environmentally friendly method for the carbon coating of aluminum is described for the first time, thus enabling high-performance LTO anodes.

Finally, a better performance is obtained using Al GnP instead of Al CB. SEM images of LTO electrodes with Al CB and Al GnP are shown in Fig. 7 to interpret this phenomenon. A planar interface between the carbon black coating and the active coating is visible (Fig. 7a). In contrast, an intensive cross-linking between the GnP coating and the active layer is observed (Fig. 7b). The GnPs are extended into the active coating, resulting in a better electrical contact between these layers compared to the utilization of CB as conductive additive in the carbon coating. Besides, Vedder et al. assert that a longer interaction between aluminum and water leads to the formation of a thicker hydroxide layer [41]. The contact time to the water used as solvent during the pre-coating varied between Al CB and Al GnP, as the drying times differed. Due to its higher surface roughness (see Table 1), Al GnP dried faster, resulting presumably in a slightly thinner hydroxide film on the aluminum surface and, as a consequence, in a better electrical contact between the aluminum, the hydroxide layer, and the carbon coating.

3.4.3 Influence of the polymer binder

The influence of the polymer binders used for the tape casting of the active mass was examined, using the example of untreated and GnP-coated aluminum current collectors. Again, anodes cast on copper served as a reference.

The capacities of these LTO anodes at different C rates are shown in Fig. 8a–c. In case of the electrodes based on a copper current collector (Fig. 8a), there are only slight deviations using different polymer binders. A similar trend is observed when Al GnP is used as current collector (Fig. 8c). The initial capacity is between 155 and 160 mAh g^{-1} in any case. Up to 1 C, the current density does not markedly affect the capacity. During cycling at 1 C, no severe degradation is observed, because of the negligible volume change of LTO during cycling [4] preventing mechanical stress within the electrode structure. Finally, even at a very high C rate (16 C), the capacity retention is between 120 and 150 mAh g^{-1}. It increases in the order: PVDF electrode—PAA electrode—Na-CMC electrode.

In case of the copper current collector, there was no insulating passive film on the metal surface which limited the electrochemical performance. Furthermore, a good

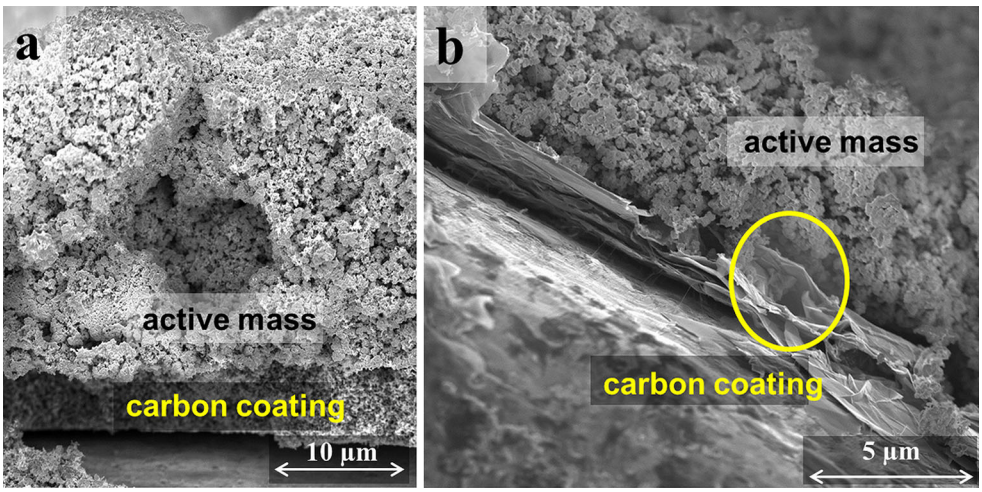

Fig. 7 SEM images of LTO electrodes with PVDF binder cast on **a** Al CB and **b** Al GnP

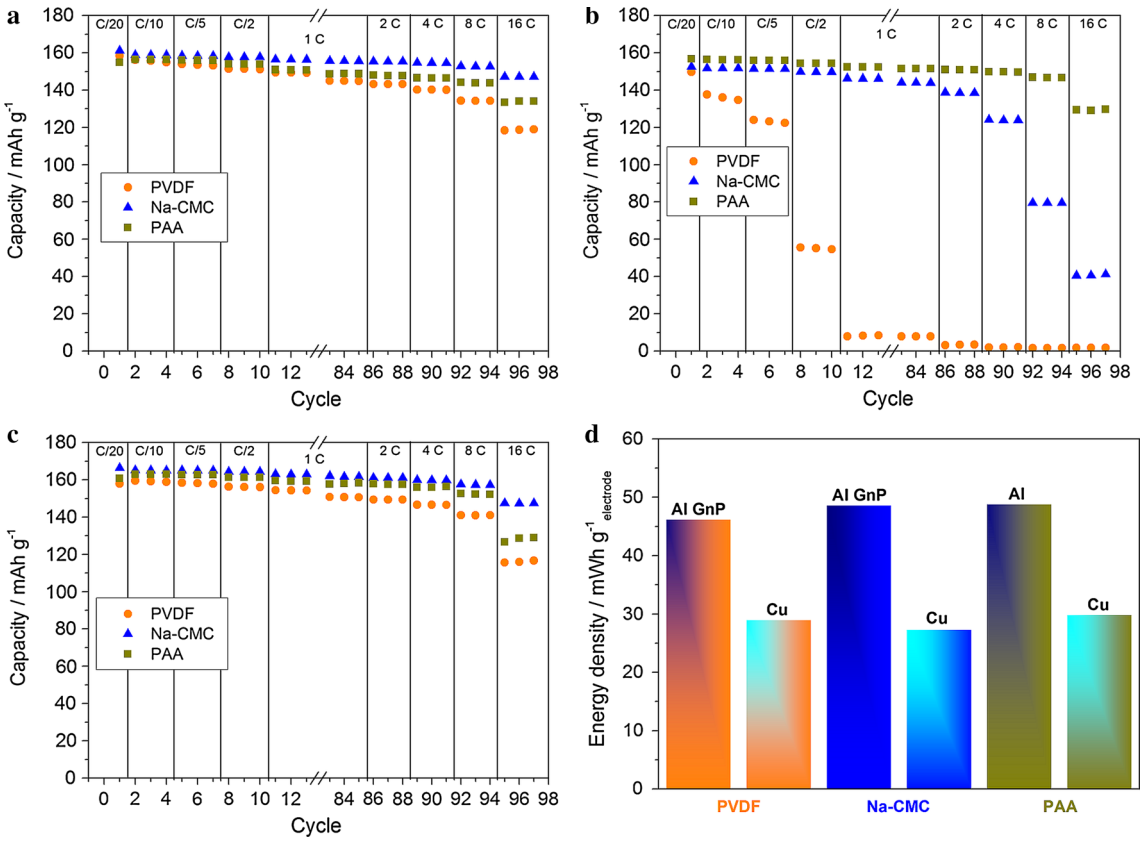

Fig. 8 Electrochemical performance of LTO electrodes depending on the applied binder: **a** capacity retention at different C rates using Cu as current collector, **b** capacity retention at different C rates with an Al current collector, **c** capacity retention at different C rates with an Al GnP current collector and **d** specific energy density, referred to the whole mass of the electrode, at 1 C depending on different current collectors

electrical contact between Al GnP and the corresponding active coatings was realized in any case. Thus, the observed differences in the capacity, especially at high C rates, are due to the structure of the active coating rather than due to the contact between active mass and current collector.

Using aqueous binder systems (see Fig. 9a, b), the active coating is more compact and homogeneous compared to

the PVDF electrode (see Fig. 9c). Various published works confirm this observation [18–20, 23]. Additionally, the electrode with the PVDF binder shows multiple agglomerates (see markings, Fig. 9a1 and a2). In contrast, fewer agglomerates are formed when using aqueous binders. Active material agglomerates were the reason for a poor rate capability, because they impede the electrolyte penetration and the electronic contact within the clusters.

Nevertheless, the electrode processed with PAA gives a slightly lower capacity than that with Na-CMC, because the PAA electrode has fewer pores. The lower porosity limited the ionic conductivity offered by the electrolyte, which became rate determining at high currents. The observed micro-cracks on the surface of the Na-CMC electrode (see markings in Fig. 9b1) did not derogate the electrochemical performance. As a matter of principle, these effects do not depend on the current collector.

Nevertheless, using aluminum as a current collector, the electrical contact between aluminum and the active mass dominated the electrode performance. In contrast to PVDF, Na-CMC and PAA were processed in aqueous solutions, causing chemical reactions between aluminum and water during the electrode casting process. That is exactly the reason why, depending on the applied polymer, the influence of the aqueous binders was so pronounced in the case of untreated aluminum, which is susceptible to chemical reactions with aqueous solutions (Fig. 8b). While the initial capacity of the LTO anodes is comparable, between 150 and 155 mAh g^{-1}, the rate capability distinctly differs. It is far worst when PVDF was applied as binder, but already remarkably improved when used Na-CMC and further enhanced in a PAA system. In the latter system, the capacity at 1 C still ranges between 145 and 150 mAh g^{-1}, being comparable to the results of Pohjalainen et al. [26]. Using PAA binder, about 130 mAh g^{-1} are measured at 16 C. This improved performance indicates an enhanced electrical contact between the PAA active coating and the aluminum current collector compared to the Na-CMC coating and aluminum. The IR spectroscopic measurements (see Fig. 4) proved that only a layer of aluminum(III)-polyacrylate forms on the metal surface when using PAA. The formation of a hydroxidic/oxyhydroxidic layer was almost completely prevented in the presence of an acidic aqueous PAA solution. Consequently, the aluminum(III)-polyacrylate film is apparently better electron permeable than the hydroxide layer formed during the casting process of the Na-CMC electrode, resulting in the observed high capacities over the whole C rate range. Additionally, the performance of the LTO anodes with a PAA binder cast on Al GnP as well as on Al is comparable (see Fig. 8b, c). Hence, a carbon coating of aluminum is not necessary to obtain a high-rate capable electrode.

In contrast, the anode processed with Na-CMC exhibits a different behavior at higher C rates depending on the current collector (Fig. 8b, c). The electrode with the untreated aluminum (Fig. 8b) yields about 40 mAh g^{-1} at 16 C, whereas the sample with Al GnP achieves a capacity of approximately 150 mAh g^{-1} at 16 C (Fig. 8c). Due to a

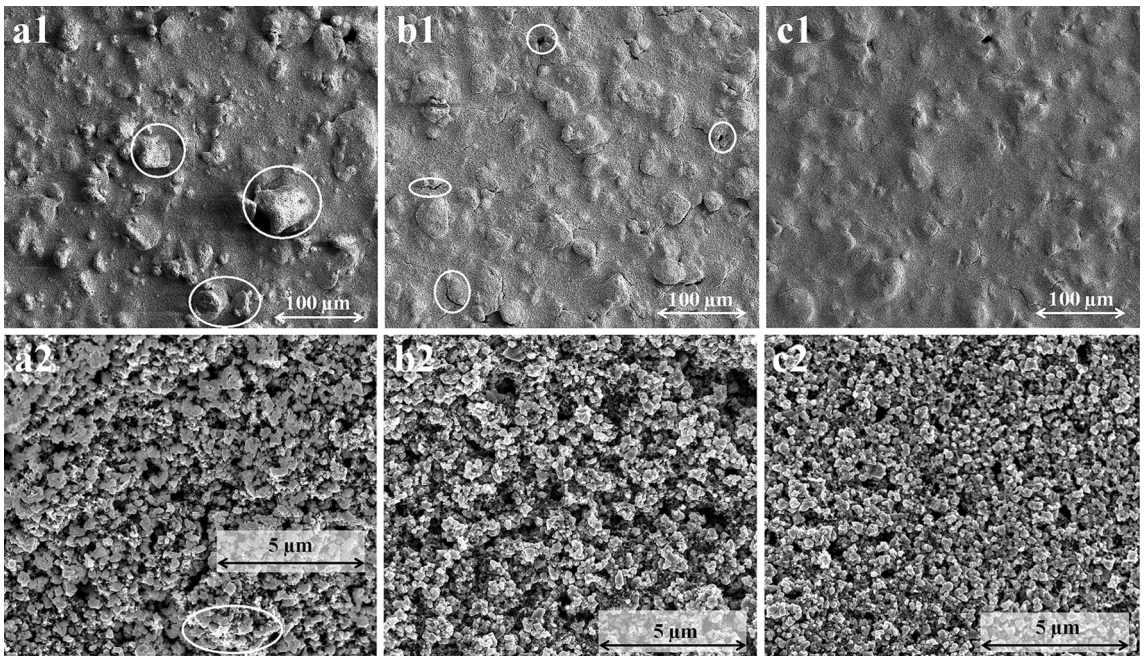

Fig. 9 SEM images of $Li_4Ti_5O_{12}$ electrodes with different binders: **a** PVDF, **b** Na-CMC and **c** PAA, and different magnifications: *1* ×300 and *2* ×10,000

thinner passive film, a higher rate capability generally indicates a better electric contact to the active mass. By applying a carbon coating on aluminum, the metal surface was protected against the aluminum–water reaction during the electrode processing. Hence, the hydroxide/oxyhydroxide layer was most likely of negligible thickness (see Sect. 3.4.2) [41], resulting in a high discharge capacity of the electrode with Al GnP. Consequently, a good electrical contact between the Na-CMC-based active mass and Al GnP was achieved. In contrast, the capacity at C rates ≥ 2 of the electrode with untreated aluminum was apparently limited by a thicker hydroxide/oxyhydroxide layer [41], which was generated during the preparation of the electrode.

Figure 8d depicts the energy density of LTO anodes depending on the binder cast on different current collectors. It has to be emphasized that for all binder systems, the energy density is enhanced by at least 59 % by substituting the heavy copper by lightweight aluminum foils, either carbon coated or untreated. Consequently, in all cases, copper can well-founded be substituted by the newly developed carbon-coated aluminum foils. In combination with the PAA binder, even untreated aluminum can serve as a current collector. Hence, a high-rate capable PAA electrode can be manufactured by a very simple and cost-effective procedure.

4 Conclusion

The performance of $Li_4Ti_5O_{12}$ electrodes depending on different current collectors and binders was studied. The investigated aluminum current collectors were carbon coated using carbon black and graphene nanoplatelets as conductive additives and Na-CMC as a binder. The coating was done by an inexpensive and environmentally friendly screen printing process. PVDF, Na-CMC as well as PAA served as binder polymers for the active mass coatings.

Based on the electrochemical measurements along with the applied analytical methods, the authors could interpret the improved performance of electrodes with treated Al foils and an aqueous binder.

- The electrical insulating native passive layer on the aluminum surface impedes the electron transfer between the PVDF coating and aluminum, resulting in a poor electrochemical performance.
- In presence of Na-CMC, the oxide of the native passive layer on aluminum is substituted by hydroxide/oxyhydroxide species, while PAA formed polyacrylate complexes on the aluminum surface. Therefore, the electrode performance is enhanced using aqueous binders. The electron permeability of the polyacrylate complexes is better than of the hydroxide/oxyhydroxide layer formed during the electrode casting process, resulting in an improved rate capability of the PAA electrode.
- In the course of the carbon coating of aluminum, (i) the native passive film was removed and (ii) the thickness of the hydroxide layer was limited as well as the aluminum surface was protected against further hydroxide/oxyhydroxide formation during the electrode casting process with the Na-CMC slurry. Therefore, the resistance between aluminum and the active mass remarkably decreased, causing an enhanced high rate capability of the PVDF as well as the Na-CMC electrode.
- The electrochemical performance of LTO electrodes processed with a copper current collector is dominated by the electrode structure. The electrodes fabricated with aqueous binder systems were more compact compared to PVDF, resulting in a higher capacity. Fewest pores were obtained for the PAA electrode, limiting the ionic conductivity within the electrode at high C rates and, consequently, the capacity.

Finally, the energy density of LTO electrodes was increased by at least 59 % by substituting the heavy copper by lightweight, carbon-coated aluminum foils. By using PAA as binder, even untreated aluminum could act as current collector.

The costly and heavy copper as well as the toxic and expensive binder system PVDF/NMP could be substituted by carbon-coated aluminum foils and aqueous binder systems. To achieve a special high-rate capable electrode, the authors suggest the utilization of Al GnP as a current collector and Na-CMC as a binder. If a simple electrode manufacturing process is preferred, the PAA binder is the best alternative, because a pre-treatment of aluminum could be circumvented.

Acknowledgments This work was financially supported by the federal ministry of education and research within the framework of the WING program (Project number: 03X0112A) and by the AiF framework (Project number: 16958N). In addition, the authors want to thank D. Kurz and A. Mingers (MPI für Eisenforschung Düsseldorf) for performing the ICP-OES experiments. Furthermore, the authors want to thank Prof. C. Schulz and Dr. H. Wiggers (Institute for Combustion and Gasdynamics (IVG), University of Duisburg-Essen) for providing the biologic VMP 3 potentiostat to measure the CVs of the current collectors.

References

1. Armand M, Tarascon J (2008) Building better batteries. Nature 451:652–657. doi:10.1038/451652a
2. Goodenough JB, Kim Y (2010) Challenges for rechargeable Li batteries. Chem Mater 22:587–603. doi:10.1021/cm901452z

3. Ohzuku T (1995) Zero-Strain insertion material of $Li[Li_{1/3}Ti_{5/3}]O_4$ for rechargeable lithium cells. J Electrochem Soc 142:1431. doi:10.1149/1.2048592
4. Sorensen EM, Barry SJ, Jung H, Rondinelli JM, Vaughey JT, Poeppelmeier KR (2006) Three-dimensionally ordered macroporous $Li_4Ti_5O_{12}$: effect of wall structure on electrochemical properties. Chem Mater 18:482–489. doi:10.1021/cm052203y
5. Zaghib K, Simoneau M, Armand M, Gauthier M (1999) Electrochemical study of $Li_4Ti_5O_{12}$ as negative electrode for Li-ion polymer rechargeable batteries. J Power Sources 81–82:300–305. doi:10.1016/S0378-7753(99)00209-8
6. Kinoshita S, Kotato M, Sakata Y, Ue M, Watanabe Y, Morimoto H et al (2008) Effects of cyclic carbonates as additives to γ-butyrolactone electrolytes for rechargeable lithium cells. J Power Sources 183:755–760. doi:10.1016/j.jpowsour.2008.05.035
7. Xu W, Chen X, Wang W, Choi D, Ding F, Zheng J et al (2013) Simply AlF_3-treated $Li_4Ti_5O_{12}$ composite anode materials for stable and ultrahigh power lithium-ion batteries. J Power Sources 236:169–174. doi:10.1016/j.jpowsour.2013.02.055
8. Bruce PG, Scrosati B, Tarascon J (2008) Nanomaterials for rechargeable lithium batteries. Angew Chem Int Ed 47:2930–2946. doi:10.1002/anie.200702505
9. Chen CH, Vaughey JT, Jansen AN, Dees DW, Kahaian AJ, Goacher T et al (2001) Studies of Mg-Substituted $Li_{4-x}Mg_xTi_5O_{12}$ Spinel Electrodes ($0 \leq x \leq 1$) for lithium batteries. J Electrochem Soc 148:A102. doi:10.1149/1.1344523
10. Ouyang C, Zhong Z, Lei M (2007) Ab initio studies of structural and electronic properties of $Li_4Ti_5O_{12}$ spinel. Electrochem Commun 9:1107–1112. doi:10.1016/j.elecom.2007.01.013
11. Fang W, Cheng X, Zuo P, Ma Y, Yin G (2013) A facile strategy to prepare nano-crystalline $Li_4Ti_5O_{12}$/C anode material via polyvinyl alcohol as carbon source for high-rate rechargeable Li-ion batteries. Electrochim Acta 93:173–178. doi:10.1016/j.electacta.2013.01.112
12. Zhang C, Zhang Y, Wang J, Wang D, He D, Xia Y (2013) $Li_4Ti_5O_{12}$ prepared by a modified citric acid sol–gel method for lithium-ion battery. J Power Sources 236:118–125. doi:10.1016/j.jpowsour.2013.01.135
13. Wu D, Cheng Y (2013) Enhanced high-rate performance of submicro $Li_4Ti_{4.95}Zn_{0.05}O_{12}$ as anode material for lithium-ion batteries. Ionics 19:395–399. doi:10.1007/s11581-012-0777-x
14. Wang G, Yan K, Yu Z, Qu M (2010) Facile synthesis and high rate capability of $Li_4Ti_5O_{12}$/C composite materials with controllable carbon content. J Appl Electrochem 40:821–831. doi:10.1007/s10800-009-0065-2
15. Xu J, Chou S, Gu Q, Liu H, Dou S (2013) The effect of different binders on electrochemical properties of $LiNi_{1/3}Mn_{1/3}Co_{1/3}O_2$ cathode material in lithium ion batteries. J Power Sources 225:172–178. doi:10.1016/j.jpowsour.2012.10.033
16. Guerfi A, Kaneko M, Petitclerc M, Mori M, Zaghib K (2007) $LiFePO_4$ water-soluble binder electrode for Li-ion batteries. J Power Sources 163:1047–1052. doi:10.1016/j.jpowsour.2006.09.067
17. Lux SF, Balducci A, Schappacher FM, Passerini S, Winter M (2010) (Invited) Na-CMC as Possible Binder for $LiFePO_4$. ECS Trans 25:265–270. doi:10.1149/1.3393862
18. Lux SF, Schappacher F, Balducci A, Passerini S, Winter M (2010) Low cost, environmentally benign binders for lithium-ion batteries. J Electrochem Soc 157:A320. doi:10.1149/1.3291976
19. Mancini M, Nobili F, Tossici R, Wohlfahrt-Mehrens M, Marassi R (2011) High performance, environmentally friendly and low cost anodes for lithium-ion battery based on TiO_2 anatase and water soluble binder carboxymethyl cellulose. J Power Sources 196:9665–9671. doi:10.1016/j.jpowsour.2011.07.028
20. Moretti A, Kim G, Bresser D, Renger K, Paillard E, Marassi R et al (2013) Investigation of different binding agents for nanocrystalline anatase TiO_2 anodes and its application in a novel, green lithium-ion battery. J Power Sources 221:419–426. doi:10.1016/j.jpowsour.2012.07.142
21. Kim G, Jeong S, Joost M, Rocca E, Winter M, Passerini S et al (2011) Use of natural binders and ionic liquid electrolytes for greener and safer lithium-ion batteries. J Power Sources 196:2187–2194. doi:10.1016/j.jpowsour.2010.09.080
22. Chou S, Wang J, Liu H, Dou S (2011) Rapid synthesis of $Li_4Ti_5O_{12}$ microspheres as anode materials and its binder effect for lithium-ion battery. J Phys Chem C 115:16220–16227. doi:10.1021/jp2039256
23. Cai Z, Liang Y, Li W, Xing L, Liao Y (2009) Preparation and performances of $LiFePO_4$ cathode in aqueous solvent with polyacrylic acid as a binder. J Power Sources 189:547–551. doi:10.1016/j.jpowsour.2008.10.040
24. Chong J, Xun S, Zheng H, Song X, Liu G, Ridgway P et al (2011) A comparative study of polyacrylic acid and poly(vinylidene difluoride) binders for spherical natural graphite/$LiFePO_4$ electrodes and cells. J Power Sources 196:7707–7714. doi:10.1016/j.jpowsour.2011.04.043
25. Lee J, Kim J, Kim YC, Zang DS, Paik U (2008) Dispersion properties of aqueous-based $LiFePO_4$ pastes and their electrochemical performance for lithium batteries. Ultramicroscopy 108:1256–1259. doi:10.1016/j.ultramic.2008.04.027
26. Pohjalainen E, Räsänen S, Jokinen M, Yliniemi K, Worsley DA, Kuusivaara J et al (2013) Water soluble binder for fabrication of $Li_4Ti_5O_{12}$ electrodes. J Power Sources 226:134–139. doi:10.1016/j.jpowsour.2012.10.083
27. Myung S, Sasaki Y, Sakurada S, Sun Y, Yashiro H (2009) Electrochemical behavior of current collectors for lithium batteries in non-aqueous alkyl carbonate solution and surface analysis by ToF-SIMS. Electrochim Acta 55:288–297. doi:10.1016/j.electacta.2009.08.051
28. Kuksenko SP (2013) Aluminum foil as anode material of lithium-ion batteries: effect of electrolyte compositions on cycling parameters. Russ J Electrochem 49:67–75. doi:10.1134/S1023193512110080
29. Schultze J, Lohrengel M (2000) Stability, reactivity and breakdown of passive films. Problems of recent and future research. Electrochim Acta 45:2499–2513. doi:10.1016/S0013-4686(00)00347-9
30. Wu H, Lee E, Wu N, Jow TR (2012) Effects of current collectors on power performance of $Li_4Ti_5O_{12}$ anode for Li-ion battery. J Power Sources 197:301–304. doi:10.1016/j.jpowsour.2011.09.014
31. Wu H, Wu H, Lee E, Wu N (2010) High-temperature carbon-coated aluminum current collector for enhanced power performance of $LiFePO_4$ electrode of Li-ion batteries. Electrochem Commun 12:488–491. doi:10.1016/j.elecom.2010.01.028
32. Striebel K, Shim J, Sierra A, Yang H, Song X, Kostecki R et al (2005) The development of low cost $LiFePO_4$-based high power lithium-ion batteries. J Power Sources 146:33–38. doi:10.1016/j.jpowsour.2005.03.119
33. Wan Z, Cai R, Jiang S, Shao Z (2012) Nitrogen- and TiN-modified $Li_4Ti_5O_{12}$: one-step synthesis and electrochemical performance optimization. J Mater Chem 22:17773. doi:10.1039/c2jm33346e
34. Aurbach D, Talyosef Y, Markovsky B, Markevich E, Zinigrad E, Asraf L et al (2004) Design of electrolyte solutions for Li and Li-ion batteries: a review. Electrochim Acta 50:247–254. doi:10.1016/j.electacta.2004.01.090
35. Wu YP, Jiang C, Wan C, Holze R (2002) Composite materials of silver and natural graphite as anode with low sensibility to humidity. J Power Sources 112:255–260. doi:10.1016/S0378-7753(02)00392-0
36. Fu LJ, Zhang HP, Wu YP, Wu HQ, Holze R (2005) Surface active sites: an important factor affecting the sensitivity of carbon

anode material toward humidity. Electrochem Solid State Lett 8:A456–A458. doi:10.1149/1.1990047
37. Gnanamuthu RM, Lee CW (2011) Electrochemical properties of Super P carbon black as an anode active material for lithium-ion batteries. Mater Chem Phys 130:831–834. doi:10.1016/j.matchemphys.2011.08.060
38. Kong F, Kostecki R, Nadeau G, Song X, Zaghib K, Kinoshita K et al (2001) In situ studies of SEI formation. J Power Sources 97–98:58–66. doi:10.1016/S0378-7753(01)00588-2
39. Kim TK, Chen W, Chen C, Wang C (2011) Capacity contribution of the interfacial layer on anode current collectors and their electrochemical properties in Lithium ion batteries. MRS Proc. doi:10.1557/opl.2011.1066
40. He Y, Liu M, Huang Z, Zhang B, Yu Y, Li B et al (2013) Effect of solid electrolyte interface (SEI) film on cyclic performance of $Li_4Ti_5O_{12}$ anodes for Li ion batteries. J Power Sources 239:269–276. doi:10.1016/j.jpowsour.2013.03.141
41. Vedder W, Vermilyea DA (1969) Aluminum+ water reaction. Trans Faraday Soc 65:561–585. doi:10.1039/TF9696500561
42. Kloprogge JT, Ruan HD, Frost RL (2002) Thermal decomposition of bauxite minerals: infrared emission spectroscopy of gibbsite, boehmite and diaspore. J Mater Sci 37:1121–1129. doi:10.1023/A:1014303119055
43. Müller B, Schmelich T (1994) Korrosionsinhibierung bzw. -stimulation von Aluminiumpigmenten im alkalisch wäßrigen Medium durch Polyacrylsäuren. Mater Corros 45:637–640. doi:10.1002/maco.19940451202
44. Müller B (1999) Polymeric corrosion inhibitors for aluminium pigment. React Funct Polym 39:165–177. doi:10.1016/S1381-5148(97)00179-X
45. Amin MA, EI-Rehim SSA, El-Sherbini EE, Hazzazi OA, Abbas MN (2009) Polyacrylic acid as a corrosion inhibitor for aluminium in weakly alkaline solutions. Part I: weight loss, polarization, impedance EFM and EDX studies. Corros Sci 51:658–667. doi:10.1016/j.corsci.2008.12.008
46. Zhu G, Liu H, Zhuang J, Wang C, Wang Y, Xia Y (2011) Carbon coated nano-sized $Li_4Ti_5O_{12}$ nanoporous micro-sphere as anode material for high-rate lithium-ion batteries. Energy Environ Sci 4:4016–4022. doi:10.1039/C1EE01680F
47. Yao XL, Xie S, Nian HQ, Chen CH (2008) Spinel $Li_4Ti_5O_{12}$ as reversible anode material down to 0 V. J Alloy Compd 465:375–379. doi:10.1016/j.allcom.2007.10.113
48. Park J, Lee S, Kim S, Kim J (2012) Effect of conductive additives on the structural and electrochemical properties of $Li_4Ti_5O_{12}$ spinel. Bull Korean Chem Soc 33:4059–4062. doi:10.5012/bkcs.2012.33.12.4059
49. Shenouda AY, Murali K (2008) Electrochemical properties of doped lithium titanate compounds and their performance in lithium rechargeable batteries. J Power Sources 176:332–339. doi:10.1016/j.jpowsour.2007.10.061